Journal Name

COMMUNICATION

Dithieno[3,2-*b*:2',3'-*d*]arsole-containing conjugated polymers in organic photovoltaic devices

Received 00th January 20xx,
Accepted 00th January 20xx

DOI: 10.1039/x0xx00000x

www.rsc.org/

Joshua P. Green,[a,†] Hyojung Cha,[a] Munazza Shahid,[a] Adam Creamer,[a] James R. Durrant,[a] and Martin J. Heeney*[,a]

Arsole-derived conjugated polymers are a relatively new class of materials in the field of organic electronics. Herein, we report the synthesis of two new donor polymers containing fused dithieno[3,2-*b*:2',3'-*d*]arsole units and report their application in bulk heterojunction solar cells for the first time. Devices based upon blends with $PC_{71}BM$ display high open circuit voltages around 0.9V and demonstrate power conversion efficiencies around 4%.

Research into new conjugated polymers for use in organic electronics applications such as organic photovoltaics (OPVs), organic field effect transistors (OFETs), and organic light emitting diodes (OLEDs) has often focussed on the use of heavier atoms as replacements for common elements such as carbon, nitrogen, oxygen, and sulfur. Examples include the use of silicon and germanium from group 14 to replace carbon, selenium and tellurium from group 16 to replace sulfur, and phosphorus from group 15 to replace nitrogen.[1–7] In general, materials containing heavy atoms have shown pronounced differences in important characteristics such as band gap, energy level, and solid-state packing when compared to their lighter analogues,[8] as well as improved efficiency of intersystem crossing leading to rapid conversion of excited state singlets to triplets,[9,10] and in some instances, solid-state phosphorescence.[11–13]

A common example of the use of heavy atoms is in the class of materials known as dithienoheteroles, in which two thiophene rings are fused by a bridging heteroatom to form a tricylic structure. Dithienoheteroles utilizing heavy bridging atoms such as silicon, germanium, and tin have been reported,[14–18] while those containing the group 15 elements nitrogen and phosphorus, especially dithieno[3,2-*b*:2',3'-*d*]pyrroles and dithieno[3,2-*b*:2',3'-*d*]phospholes (DTPs) have seen use in many areas of organic electronics.[19–21] Dithienophospholes in particular exhibit a number of interesting properties that make them potentially useful candidates for use in OPV devices, including a high degree of optoelectronic tunability via the alteration of the exocyclic groups.[22–25] For example, Park et al. have reported a promising donor co-polymer of a DTP-oxide and a dithienyl-benzo[1,2-*b*:4,5-*b*']dithiophene (BDT) which exhibited power conversion efficiencies (PCEs) of up to 6.10% in blends with phenyl-C_{61}-butyric acid methyl ester (PCBM).[26] However, the vast majority of work relating to DTP units has focused on those containing pentavalent phosphorus atoms, and there has been little exploration of the properties of DTPs containing trivalent phosphorus. This is likely due to the oxygen-sensitivity of organophosphorus atoms in the +3 oxidation state, which can lead to rapid and or uncontrolled oxidation of materials under atmospheric conditions.

It has recently been reported that the arsenic analogues of phospholes, commonly referred to as arsoles, show greatly improved oxygen stability in the +3 oxidation state at the expense of a slight reduction in aromaticity.[27–31] This has been utilised to prepare several materials containing trivalent As atoms, including a few examples of conjugated polymers.[32–37] We have previously reported that a polymer containing dithieno[3,2-*b*:2',3'-*d*]arsole (DTAs) demonstrated promising performance in OFET devices, combining good air stability with a hole mobility of 0.08 $cm^2V^{-1}s^{-1}$.[38] Building on this work, we herein describe the synthesis of novel donor polymers containing DTAs and report their application in OPV devices. To the best of our knowledge, this is the first time that DTAs containing polymers have been employed in solar cell devices. Although the overall power conversion efficiency (PCE) is lower than current state-of-the-art donor polymers, this first example nevertheless demonstrates that heavy analogues can afford useful device efficiency, with ample opportunity for future optimisation

[a] *Department of Chemistry, Imperial College London, London, SW7 2AZ, U.K.*
† Current address: Synthetic Molecular Chemistry, Department of Chemistry Ångström Laboratories, Uppsala University, Box 523, 751 20 Uppsala, Sweden
Electronic Supplementary Information (ESI) available: [details of any supplementary information available should be included here]. See DOI: 10.1039/x0xx00000x

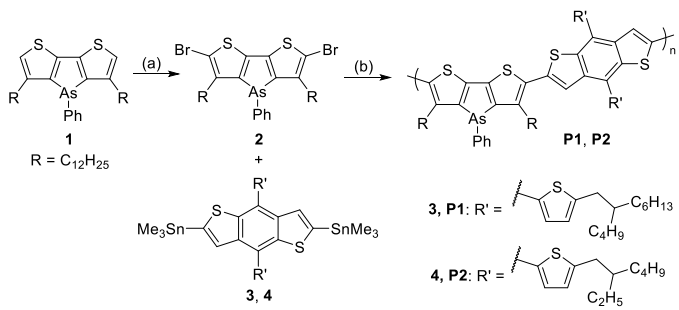

Figure 1: Synthesis of dithienoarsole monomer **2** and polymerisation with 2D-BDTs **3** and **4**. Reaction conditions: (a) 3.1 eq. lithium diisopropylamide, –78→–30→–78 °C, 4 eq. CBr_4; (b) $Pd(PPh_3)_4$, chlorobenzene, microwave reactor

Our starting point was the peripherally alkylated DTAs unit, **1**, which was prepared according to the previously reported route.[38] We note that **1** contains long linear dodecyl chains in order to promote solubility of the resulting polymer. Compound **1** was converted to the dibromo compound **2**, by dilithiation at the 2 and 6 positions using lithium diisopropylamine (LDA) followed by quenching with CBr_4 to yield **2**. This was polymerised with two different stannylated benzodithiophene (BDT) derivatives (**3** and **4**) via Stille coupling in a microwave reactor to yield polymers **P1** and **P2**.

The BDT comonomers were chosen because the peripheral thiophene groups on the BDT allow two-dimensional conjugation to be extended onto the side chains, potentially lowering the band gap of the resulting polymers and providing improvements in OPV device characteristics.[39,40] This strategy has been utilized by a number of researchers to enhance OPV performance.[41–43] In our case, we utilised two different solubilising groups on the thienyl groups of the BDT in order to both control polymer solubility and influence the thin film morphology of the solar cell blend.

In our initial attempt with co-monomer **3**, the resulting polymer **P1** was highly soluble, such that the entire polymer was extracted into the hexane during attempted purification by solvent extraction. This complicated the removal of low molecular weight oligomers, which are known to be detrimental to device performance.[15,44] Therefore shorter 2-ethylhexyl chains were used on co-monomer **4** instead to improve the effectiveness of the Soxhlet separation on **P2**. This was only partially successful since hexane extraction still removed a significant portion of the polymer (84% yield). Nevertheless, a small percentage of higher weight polymer was isolated as a chloroform-soluble fraction (7% yield).

The molecular weight, as measured by gel permeation chromatography against polystyrene standards, is shown in **Table 1**, demonstrating that despite the high solubility in hexane, both polymers had a reasonable molecular weight. As expected the $CHCl_3$ fraction of **P2** was significantly higher molecular weight than the hexane fraction. The structures of the polymers were confirmed by ^1H NMR and elemental analysis, both of which were in good agreement with expected structure. We note that no evidence of arsole oxidation was apparent by ^1H NMR.[38] Both polymers were soluble in a wide range of chlorinated and non-chlorinated organic solvents, including chloroform, chlorobenzene, toluene, hot THF, and hot hexane (hexane fractions only). No obvious thermal transitions were observed by differential scanning calorimetry up to 300 °C (Figure S1).

Table 1: Summary of molecular weight information for polymers, as measured by GPC in chlorobenzene (80 °C) *vs* polystyrene standards

	FRACTION	YIELD	M_n (Kg/mol)	M_w (Kg/mol)	$Đ$
P1	Hexane	93.5%	14.0	27.0	1.93
P2	Hexane	83.7%	20.0	37.2	1.86
P2	$CHCl_3$	7.3%	30.0	50.4	1.68

The absorption spectra of the hexane fractions of the two polymers both in chlorobenzene solutions and as thin films spun from chloroform are shown in **Figure 2** (note: the optical and electronic properties of the chloroform fraction of **P2** were not studied due to the low amount of material recovered). Both polymers were relatively wide band gap, and the solution spectra were similar, with the slightly higher molecular weight of **P2** resulting in a minor red shift from 507 nm to 511 nm, and an earlier onset of absorption at ~620 nm instead of ~580 nm, possibly indicating a small amount of aggregated material in solution. In the thin film spectra, the λ_{max} of both polymers was red-shifted compared to solution, due to planarization of the backbone in the solid state, with very minor differences in λ_{max} observed (**P1** at 539 nm and **P2** at 536 nm). Both polymers also showed intense shoulders at 577 nm, likely due to aggregation of the backbone in the thin film state. Annealing the films 120 °C did not change the shape of the spectra.

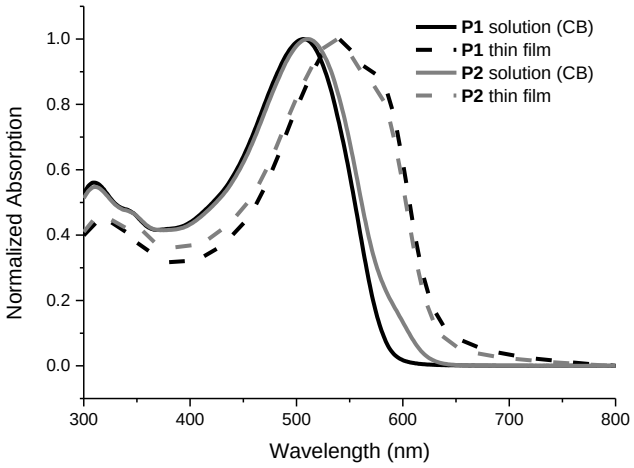

Figure 2: UV/vis absorption spectra of hexane fractions of **P1** and **P2** in chlorobenzene solutions and as thin films

The electrochemical properties of the two polymers were studied using cyclic voltammetry (CV) and photoelectron spectroscopy in air (PESA). The CVs of the two polymers show irreversible oxidation peaks that indicate oxidation potentials of −5.33 and −5.34 eV for **P1** and **P2**, respectively (referenced against ferrocene/ferrocenium and measured from the onsets of oxidation – see Figure S2 and S3). The onsets of the reduction

peaks were also measured from pristine films, with electron affinities of −3.22 and −3.26 eV for **P1** and **P2**, respectively, giving electrochemical band gaps of 2.11 eV for **P1** and 2.08 eV for **P2**. These values are within the experimental error of CV of each other (±0.1 eV), indicating that altering the alkyl chains did not substantially change the electrochemical properties of the polymers, in line with expectations. The ionisation potentials of spun-cast thin films of the polymers were also measured using PESA. In this case, the ionisation potentials were 5.22±0.05 eV for **P1** and 5.19±0.05 eV for **P2**. Hence the two polymers were within experimental error of each other and were relatively close to the oxidation potentials as observed using CV.

The photovoltaic performance of both polymers was investigated in bulk heterojunction devices with conventional architectures (ITO/PEDOT:PSS/active layer/Ca/Al), while **P2** was also tested in inverted cells (ITO/ZnO/Active layer/MoO_3/Ag). $PC_{71}BM$ was used as the acceptor due to its improved absorption in the visible region over $PC_{60}BM$. As a starting point for the optimisation, we used the conditions developed by Park and coworkers for a structurally similar **DTP-oxide** co-polymer, in which a 1:4 blend of polymer:$PC_{71}BM$ was used together with 1,8-octanedithiol (see table S1).[26] After some optimisation we found that slightly lower ratios of PCBM gave the best performance, with the optimal ratio being 1:3. For **P1** the best performance was obtained from spun-cast blends in 1,2-dichlorobenzene (DCB) without any 1,8-octanedithiol or annealing steps, whilst **P2** benefitted from a thermal annealing step at 120 °C after spin coating of the active layer. **Table 2** summarises the best device characteristics obtained for the two polymers. We note that a relatively large spread in device performance was observed, which we believe was related to the poor wetting of the blend on the hydrophilic PEDOT:PSS. This may relate to the high alkyl chain density in the polymer backbones. Devices fabricated using **P2** clearly showed improved performance compared to the butyloctyl-containing alternative, **P1**. Indeed, even the best performing **P1** device gave a lower PCE than the average of the **P2** cells, at 2.45% and 2.86%, respectively. The improved performance of **P2** may be related to the higher molecular weight of the hexane fraction since this is known to have a significant impact on device performance.

Table 2: Photovoltaic performances and device characteristics for **P1** and **P2**.

	P1[b]	P2[b]	P2 (inverted)[c]
V_{oc} (V)	0.76±0.03	0.83±0.01	0.91±0.01
J_{sc} (mA cm^{-2})	7.43±0.85	7.16±2.25	9.50±0.10
FF	0.37±0.03	0.48±0.01	0.44±0.01
PCE (%)[a]	2.11±0.21 (2.45)	2.86±0.9 (4.04)	3.80±0.10 (3.90)

[a] Maximum PCE is given in parentheses after the average value. Average data and standard deviation obtained from six[b] and eight[c] devices

Based on the more promising performance of **P2**, this was investigated further in inverted OPV devices (ITO/ZnO/Active layer/MoO_3/Ag) using the same coating conditions. The wetting of the film on the ZnO layer was visually better than on the PEDOT:PSS of the conventional devices, resulting in less variation in device performance. Overall, similar performance was obtained (**Table 2**) for the as-cast device compared to the best conventional devices. In this case, thermal annealing did not result in any further device improvements. The J-V characteristics and EQE are shown in Fig 3. The EQE demonstrates that due to the high PCBM loading, the bulk of the current generation is from the high energy wavelength region (400–500 nm), but nevertheless there is clear current generation from the donor region at longer wavelengths. Although the overall device efficiency is moderate compared to state-of-the-art donors, the cells exhibit reasonable performance for a wide band gap donor, with high open circuit voltages observed. It demonstrates for the first time that arsole containing polymers are capable of generating charge in a photovoltaic device. Further optimization of device performance by tuning of the alkyl sidechains and co-monomers to control the blend microstructure should be possible.

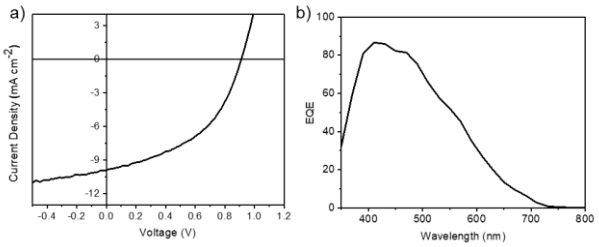

Figure 3: a) J-V curve of inverted OPV device prepared using **P2:$PC_{71}BM$** in the active layer. b) EQE curve for inverted **P2:$PC_{71}BM$** device.

Conclusions

In summary, we have reported the synthesis of two new dithienoarsole containing co-polymers by Stille polymerisation. The polymers, which differ only in the length of their alkyl sidechains, were highly soluble in organic solvents and display good ambient stability in the +3 oxidation state. Organic solar cell devices based on blends of the polymers with $PC_{71}BM$ exhibited notable differences depending on the length of the alkyl sidechain. Power conversion efficiencies around 4% with high open circuit voltages were obtained for the inverted device architectures. To the best of our knowledge, this is the first report of an arsole-containing polymer in a photovoltaic device, and it further highlights the potential of such materials in electronic devices.

Conflicts of interest

There are no conflicts to declare.

Acknowledgements

We thank the EPSRC (EP/G037515/1) and the Daphne Jackson Trust (supported by RSC and EPSRC) for financial support.

Notes and references

1 A. M. Priegert, B. W. Rawe, S. C. Serin and D. P. Gates, *Chem. Soc. Rev.*, 2016, **45**, 922–953.
2 M. Jeffries-El, B. M. Kobilka and B. J. Hale, *Macromolecules*, 2014, **47**, 7253–7271.
3 J. Crassous and R. Réau, *Dalt. Trans.*, 2008, 6865.
4 E. I. Carrera and D. S. Seferos, *Macromolecules*, 2015, **48**, 297–308.
5 M. A. Shameem and A. Orthaber, *Chem. - A Eur. J.*, 2016, **22**, 10718–10735.
6 S. M. Parke, M. P. Boone and E. Rivard, *Chem. Commun.*, 2016, **52**, 9485–9505.
7 F. Jäkle and F. Vidal, *Angew. Chemie Int. Ed.*, , DOI:10.1002/anie.201810611.
8 X. He and T. Baumgartner, *RSC Adv.*, 2013, **3**, 11334–11350.
9 R. D. Pensack, Y. Song, T. M. McCormick, A. A. Jahnke, J. Hollinger, D. S. Seferos and G. D. Scholes, *J. Phys. Chem. B*, 2014, **118**, 2589–2597.
10 B. D. Datko, A. K. Thomas, Z. Fei, M. Heeney and J. K. Grey, *Phys. Chem. Chem. Phys.*, 2017, **19**, 28239–28248.
11 G. He, B. D. Wiltshire, P. Choi, A. Savin, S. Sun, A. Mohammadpour, M. J. Ferguson, R. McDonald, S. Farsinezhad, A. Brown, K. Shankar and E. Rivard, *Chem. Commun.*, 2015, **51**, 5444–5447.
12 S. M. Parke and E. Rivard, *Isr. J. Chem.*, 2018, **58**, 915–926.
13 J. Ohshita, S. Matsui, R. Yamamoto, T. Mizumo, Y. Ooyama, Y. Harima, T. Murafuji, K. Tao, Y. Kuramochi, T. Kaikoh and H. Higashimura, *Organometallics*, 2010, **29**, 3239–3241.
14 V. Gupta, L. F. Lai, R. Datt, S. Chand, A. J. Heeger, G. C. Bazan and S. P. Singh, *Chem. Commun.*, 2016, **52**, 8596–8599.
15 G. L. Gibson, D. Gao, A. A. Jahnke, J. Sun, A. J. Tilley and D. S. Seferos, *J. Mater. Chem. A*, 2014, **2**, 14468–14480.
16 D. Tanaka, J. Ohshita, Y. Ooyama, N. Kobayashi, H. Higashimura, T. Nakanishi and Y. Hasegawa, *Organometallics*, 2013, **32**, 4136–4141.
17 S. Urrego-Riveros, I. M. Ramirez y Medina, J. Hoffmann, A. Heitmann and A. Staubitz, *Chem. - A Eur. J.*, 2018, **24**, 5680–5696.
18 S. V. Kesava, Z. Fei, A. D. Rimshaw, C. Wang, A. Hexemer, J. B. Asbury, M. Heeney and E. D. Gomez, *Adv. Energy Mater.*, 2014, **4**, 1–10.
19 T. Baumgartner and R. Réau, *Chem. Rev.*, 2006, **106**, 4681–4727.
20 S. C. Rasmussen and S. J. Evenson, *Prog. Polym. Sci.*, 2013, **38**, 1773–1804.
21 T. Baumgartner, T. Neumann and B. Wirges, *Angew. Chemie Int. Ed.*, 2004, **43**, 6197–6201.
22 M. P. Duffy, W. Delaunay, P.-A. A. Bouit and M. Hissler, *Chem. Soc. Rev.*, 2016, **45**, 5296–5310.
23 Y. Ren, Y. Dienes, S. Hettel, M. Parvez, B. Hoge and T. Baumgartner, *Organometallics*, 2009, **28**, 734–740.
24 G. C. Welch, T. Baumgartner, T. A. Welsh, A. Laventure, T. Baumgartner and G. C. Welch, *J. Mater. Chem. C*, 2018, **6**, 2148–2154.
25 Y. J. Kim, M. J. Kim, T. K. An, Y. H. Kim and C. E. Park, *Chem. Commun.*, 2015, **51**, 11572–11575.
26 K. H. Park, Y. J. Kim, G. B. Lee, T. K. An, C. E. Park, S.-K. Kwon and Y.-H. Kim, *Adv. Funct. Mater.*, 2015, **25**, 3991–3997.
27 A. M. Gregson, S. M. Wales, S. J. Bailey and P. A. Keller, *J. Organomet. Chem.*, 2015, **785**, 77–83.
28 C. J. O'Brien, Z. S. Nixon, A. J. Holohan, S. R. Kunkel, J. L. Tellez, B. J. Doonan, E. E. Coyle, F. Lavigne, L. J. Kang and K. C. Przeworski, *Chem. - A Eur. J.*, 2013, **19**, 15281–15289.
29 J. P. Green, S. J. Cryer, J. Marafie, A. J. P. White and M. Heeney, *Organometallics*, 2017, **36**, 2632–2636.
30 J. P. Green, A. K. Gupta and A. Orthaber, *Eur. J. Inorg. Chem.*, 2019, **2019**, 1539–1543.
31 H. Imoto, T. Fujii, S. Tanaka, S. Yamamoto, M. Mitsuishi, T. Yumura and K. Naka, *Org. Lett.*, 2018, **20**, 5952–5955.
32 Y. Matsumura, M. Ishidoshiro, Y. Irie, H. Imoto, K. Naka, K. Tanaka, S. Inagi and I. Tomita, *Angew. Chemie Int. Ed.*, 2016, **55**, 15040–15043.
33 T. Kato, H. Imoto, S. Tanaka, M. Ishidoshiro and K. Naka, *Dalt. Trans.*, 2016, **45**, 11338–11345.
34 S. Tanaka, H. Imoto, T. Yumura and K. Naka, *Organometallics*, 2017, **36**, 1684–1687.
35 C. Yamazawa, H. Imoto and K. Naka, *Chem. Lett.*, 2018, **47**, 887–890.
36 H. Imoto, C. Yamazawa, S. Hayashi, M. Aono and K. Naka, *ChemElectroChem*, , DOI:10.1002/celc.201801069.
37 H. Imoto and K. Naka, *Chem. - A Eur. J.*, 2018, 1–13.
38 J. P. Green, Y. Han, R. Kilmurray, M. A. McLachlan, T. D. Anthopoulos and M. Heeney, *Angew. Chemie Int. Ed.*, 2016, **55**, 7148–7151.
39 L. Huo, S. Zhang, X. Guo, F. Xu, Y. Li and J. Hou, *Angew. Chemie Int. Ed.*, 2011, **50**, 9697–9702.
40 R. Duan, L. Ye, X. Guo, Y. Huang, P. Wang, S. Zhang, J. Zhang, L. Huo and J. Hou, *Macromolecules*, 2012, **45**, 3032–3038.
41 L. Huo, J. Hou, S. Zhang, H.-Y. Chen and Y. Yang, *Angew. Chemie Int. Ed.*, 2010, **49**, 1500–1503.
42 P. Sista, M. C. Biewer and M. C. Stefan, *Macromol. Rapid Commun.*, 2012, **33**, 9–20.
43 J. Hou, Z. Tan, Y. Yan, Y. He, C. Yang and Y. Li, *J. Am. Chem. Soc.*, 2006, **128**, 4911–4916.
44 Y. Li, *Acc. Chem. Res.*, 2012, **45**, 723–733.